Effects on the predominant periods due to abrupt lateral soil heterogeneities

V. Salinas, S. Santos-Assunçao, O. Caselles, V. Pérez-Gracia, Ll. G. Pujades, J. Clapés
Universidad Politécnica de Cataluña

SUMMARY
An important part of seismic risk evaluations is microzonation. Notwithstanding, narrow lateral changes could strongly affect the seismic soil response. When changes appear, a more detailed evaluation is needed. This is the case of Barcelona (NE of Spain) that is crossed by a large number of infilled torrents and paleochannels which might cause non-negligible effects in the soil response. Bad selection of representative points could lead to important deviations of the predominant period maps. Due to the previous assumptions, the objective of this work is to detect the presence of these lateral changes in Barcelona and to evaluate their effects on the predominant period values. In this work, the main results are described, by showing 3 representative cases. The resolution and reliability of the methodology is also discussed. In addition, one-dimensional soil model is fitted to data where is possible.

Keywords: HV spectral ratio; Ground Penetrating Radar; Diffuse Fields; Dense Cities; Paleochannels.

1. INTRODUCTION

From the contributions of Nakamura (Nakamura, 1989), ambient vibration H/V method has become a widely practice to measure seismic soil response in terms of predominant period values. During the last decades, microzonation maps have been carried out by relying on this method (e.g., Navarro et al., 2001; D'Amico et al., 2002; Gosar & Martinenc, 2009). Microzonation usually has been interpreted to take into account lateral soil changes of about 100 meters or more. From this point of view, microzonation has the problem of selecting a representative point for the entire microzone when unexpected geological changes are present or, moreover, if there is a representative point for this microzone. An error in this interpretation of microzonation could lead to a worst evaluation of risk analysis and, therefore, to serious problems of the structures built over the soils with non-representative soil response assigned. In case of wide urban areas this issue is of particular interest. Cities are mostly built on quaternary soils and usually characterized by lateral heterogeneous geological settings which can introduce differentiated responses in short distances (D'amico et al., 2008; Caselles et al., 2010). Then, the interest of determine the response taking into account the size of geological homogeneity dimension has lead to the concept of nanozonation (Pérez-Gracia et al., 2010).

In order to study the changes induced by these abrupt lateral heterogeneities it is important to bear in mind the strengths and limitations of the H/V ratio method (Cadet, 2007; Bard, 2008). Usually it is assumed (Pilz et al. 2009) that the site predominant period is the only reliable parameter that might be obtained by means of H/V ratio. Recent works, (Lunedei & Albarello, 2010, Sánchez-Sesma et al., 2011) can shed light on this issue. In this way, diffuse field theory (Sánchez-Sesma et al., 2011; Luzón et al., 2011) have been proved useful to understand the background of the H/V ratio. Some applications of this theory have been used to study the seismic soil response.

Barcelona is an example where the previous consideration must be done in order to obtain reliable information about seismic soil response. A great variability of dominant periods appears depending on

the geological characteristics. Sometimes this variability arises in short distances due to local structures which introduce anomalies in seismic soil response. These structures, as streams or paleochannels, often were filled with anthropogenic materials during the city urbanization processes. Some previous works about microzonation has been done in Barcelona (Cid et al., 2001; Cadet, 2011). Notwithstanding, the effect of the local heterogeneities are not taken into account in these studies. The great variability in short distances of predominant period observed in other works (Alfaro et al., 2001) may be explained by means of this kind of structures.

An accurate nanozonation could be done by performing enough measurements to detect all the significant features. Obviously, this methodology is a complicate, expensive and time-consuming process, and sometimes unviable in cities like Barcelona. An alternative methodology is to perform a previous inspection using other techniques to detect geological changes related with soil response variations. In this second methodology, the alternative techniques should determine the necessary points where measurements must be done, in order to obtain a realistic map of soil response. GPR appears as one of the best geophysical methods to obtain the necessary information, due to its quick survey and to the capability to recognize scattering. However, it is important to point out that GPR does not observes density contrasts but electromagnetic, so, changes observed in GPR data could not perfectly agree with changes in seismic soil response. Nevertheless, some previous measurements (Pérez-Gracia et al., 2010) seems to point out that changes in the GPR amplitude could be a useful tool to highlight the most complex zones. Unconsolidated soils cause more GPR energy diffraction than homogeneous media. As heterogeneities are related to a complex soil, they could be detected by the evaluation of the noise amplitude in the GPR records.

In this work, we have studied three cases where lateral variations in surface geology are expected. In each site microtremor measurements have been done in order to compute H/V ratio. Also, GPR profiles are carried out and their reflectivity is computed. In two of the sites (where possible) Refraction Microtremors (REMI) technique was applied to obtain dispersion curves of each site. At last, for these two sites a joint inversion is computed for both H/V and REMI data. Results have been compared to existing soundings close to the sites.

2. SITES

The three sites studied in the present work are situated inside Barcelona city. The city is placed in a plane (Barcelona semigraben) of about 60 km long and 16 km wide between the Mediterranean Sea (E) and Collserola-Montnegre Horst (W). Mainly the city is built on a quaternary plane but over tertiary and Paleozoic materials outcropping in the mountain side. The semigraben includes three main geological formations. The first and second studied sites are focused in the one called “tricicle” formation. The “tricicle” is composed by a succession of three facies of red clay, yellow slime and pink limestone (of about 20 centimeters of thickness) and surrounded by the Collserola and Montjuic blocks and Llobregat and Besos deltaic deposits. At the north of the city, between the Barcelona plane and the Collserola block, appears the Turons block formed by metamorphic rocks. Turons are separated of Collserola by the Sarrià-Vall d’Hebron depression which is filled by quaternary materials (Parcerisa, 2002). Our third studied zone is in the limit of Rovira’s Hill (in the Turons block) with the Vall d’Hebron depression. In this zone thin quaternary materials overlap limestone, sandstone, slate and granite sand. The two formations of our interest are widely cut by paleochannels and torrents filled by gravel, sand, clay and slate gravel. Some of these torrents have thickness bigger than 35 meters (Ventayol et al., 2000). In Barcelona there are a lot of paleochannels and infilled torrents that are not all well located. There are some historical data about lot of them (i.e. Arandes, 1998; Vazquez, 1861; Cerda, 1885) but imprecise old cartography and difficulties in historical data interpretation conduce to significant errors in accurately positioning. Also, there is a geotechnical map (Ventayol et al. 2000) of Barcelona that show the aquifer flows recognized by geotechnical procedures. There are also anthropogenic deposits in some places, especially in not geological fully-filled torrents and the scarp between this formation and the deltaic one.

We expect to find streams in the three sites under study. Even though historical data and cartography show a deviated location for these structures, it may serve as a first approximated location. Sometimes, in addition to the location errors, the previous data consider the streams as thin lines, when we are interested in the flood plane. Site 1 (Fig. 2.1.), is situated in the centre of the city over the "tricicle" formation. It is located in Mallorca Street between Enric Granados Street and Rambla Catalunya. There are a lot of soundings close to this area, one street farther where there is a train tunnel. The expected stream at this site is the one named "Rambla d'en Malla". Second site (Fig 2.1.) is located in Diagonal Avenue near Francesc Macia square. As in the previous case, the geological formation is the "tricicle" but thinner. Now, the nearest soundings were carried out when a parking was built, about 200 meters long. The expected torrent in this site corresponds to the torrent of Ballescà. Site 3 (Fig 2.1.) is in Arenys Street and is quite different to the previous two. In this case, the sedimentary layer is less than 20 meters thick and formed formed by granite sand. Here, the closest soundings are the ones obtained during the extension of the Metro line 5. The thickness of the expected torrent is the lowest one and comes from Rovira's Hill in opposite direction to the sea, jointing other greater channel called "Torrent de la Clota" in the Vall d'Hebron depression.

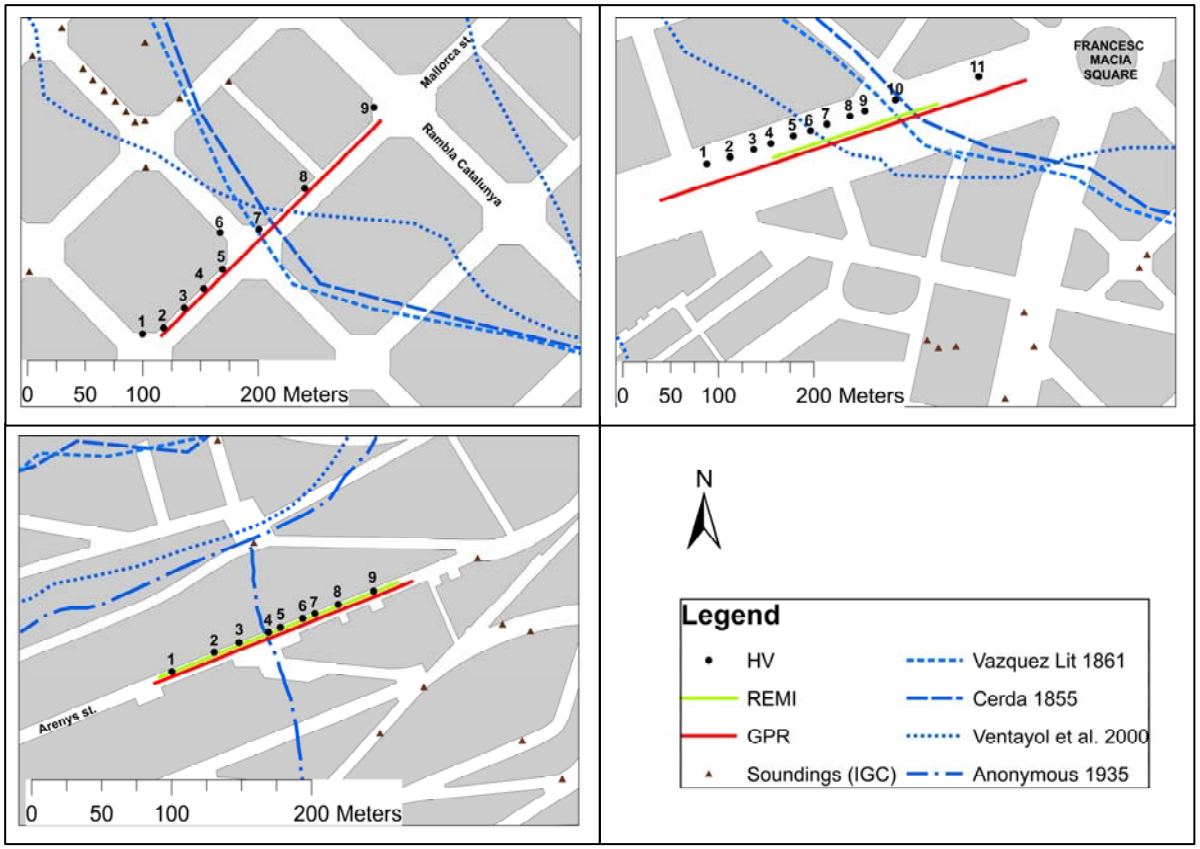

Figure 2.1. Site location. Top left: Site 1 in Mallorca Street between Enric Granados Street and Rambla Catalunya. Tor right: site 2 in Diagonal Avenue near Francesc Macia square. Bottom left: site 3 in Arenys Street. In blue: flows and torrents according to the bibliography and historical data. In brown triangles: soundings. In black dots: microtremors measurements points. In red: GPR profiles. In green: REMI arrays.

3. SURVEYS AND DATA PROCESSING

Three component records of ambient vibration noise were acquired with a low-noise seismograph at 256 sps. In site 1, recording time was 16 or 20 minute and stable windows of 16 or 32 seconds were selected depending on the expected value under SESAME project criteria (Bard, 2008). In site 2, recording time was 16 minutes and 16 second stable windows were selected in order to compute H/V. For site 3, stable windows of 8 seconds extracted from 8 minutes records were considered. In the three

cases, processing was done in a standard way and the predominant period was selected by means of a Gaussian fit. H/V curve was computed by weighting energy average of the stable windows (Caselles et al., 2010).

Multi-station microtremor survey was carried out in sites 2, and 3. REMI data was acquired by means of a 24-sensor lineal array and the sensors were spaced 8 meters. The vertical geophone had a central frequency of 4.5 Hz. In both sites, time series of 30 seconds at 500 sps were obtained. Processing and dispersion curves retrieval was done in a standard way (Louie, 2001). Time series of REMI were also used in order to validate the one-dimensional assumption of the sites, or otherwise, to split in more than one with homogeneous soil properties. For sites 2 and 3, a one-dimensional soil model was simultaneously fitted for H/V and dispersion curves.

At sites 1 and 2, GPR profiles were obtained through a bistatic rough terrain antenna (RTA) of 25 MHz nominal centre frequency. In site 3 case, GPR profile was obtained with a bistatic 100 MHz nominal centre frequency antenna.

4. METHODOLOGY

4.1. Applicattion of Diffuse Fields.

Recent theoretical advances (Weaver & Lobkis, 2004; Snieder, 2004; Sánchez-Sesma & Campillo, 2006, Sánchez-Sesma et al., 2006) shows that under the assumption of evenly distributed sources of noise, the Green's Function between two points may be retrieved from the cross-correlation of records obtained at these sites. The use of ambient vibration as diffuse seismic wavefield to retrieve the Green's Function has been tested for both surface (Shapiro & Campillo, 2004; Sabra et al., 2005) and body waves (Roux et al., 2005). The previous results, implies the proportionality between the average energy densities of a diffuse field and the imaginary part of GF at the source (Sánchez-Sesma et al., 2008; Perton et al., 2009).

Thus, directional energy densities (DED's) show the relation between average autocorrelations and the imaginary part of the Green function for a given direction. If we associate the autocorrelation of recorded motion of a diffuse wavefield, for each direction, we can write the H/V ratio as follows (Sánchez-Sesma et al., 2011).

$$\frac{H(\omega)}{V(\omega)} = \sqrt{\frac{\mathrm{Im}\left[G_{11}(0,0;\omega)\right] + \mathrm{Im}\left[G_{22}(0,0;\omega)\right]}{\mathrm{Im}\left[G_{33}(0,0;\omega)\right]}} = \sqrt{\frac{E_1(0,\omega) + E_2(0,\omega)}{E_3(0,\omega)}} \tag{4.1}$$

where $\mathrm{Im}\left[G_{ii}(0,0;\omega)\right]$ is the imaginary part of the Green function for *i*-direction in the receiver. In this way, we are capable to retrieve the H/V response of a certain 1D subsoil model.

On the other hand, to validate the one-dimensional assumption for REMI, we have also used diffuse field theory. The autocorrelation function of the vertical motion is the same for all sensors located in the same one-dimensional structure (Luzón et al., 2011):

$$U_3(\mathbf{x},\omega) = \sqrt{\left\langle \left| u_3(\mathbf{x},\omega) \right|^2 \right\rangle} \tag{4.2}$$

where the term on the right is directly the autocorrelation function for the motion in the vertical direction.

4.2. GPR Noise Amplitude (GPRNA)

The objective of the GPR survey was to detect anomalous ground areas due to the existence of paleochannels of torrents. These geological features are characterized by heterogeneous media, and GPR signal presents a high scattering level. In order to quantify the changes in the scattered energy along a profile, the analysis of the GPR noise is considered because this energy increases the noise level. An objective way to define the noisiest areas is to evaluate the raw data after amplitude corrections are applied. The amplitude is corrected by geometrical spreading and by soil materials absorption, as follows:

$$A = A_0 \cdot \left(0.08 \cdot t^{\alpha}\right)^{\beta} \tag{4.3}$$

where $A_0(t)$ is the amplitude of the raw data, t is the travel time, α is the geometrical spreading and β is the soil absorption. Representative values for Barcelona soil are $\alpha=0.1$ and $\beta=0.2$. The maximum of the corrected amplitudes is computed along a temporal window in order to avoid surface reflectors.

5. RESULTS

Table 1 shows the obtained predominant period in all sites. Only one peak appears in site 1 meanwhile in site 2 two clear differentiated peaks are observed. H/V curves in site 3 show more complex shape. Sometimes appear multiple peaks in periods close to each other. When possible, the two main peaks are chosen.

Table 1. Predominant periods (in seconds) obtained from microtremors in all sites.

Point	1	2	3	4	5	6	7	8	9	10	11
Site 1	1.42	1.41	1.57	1.73	1.93	1.37	1.36	1.42	1.55	-	-
Site 2	0.28	0.31	0.30	0.26	0.29	0.27	0.30	0.26	0.30	0.27	0.29
	0.94	0.86	0.82	1.25	0.94	1.11	0.89	0.89	0.93	0.89	-
Site 3	0.20	0.17	0.17	0.15	0.14	0.20	0.15	0.15	0.19	-	-
	-	0.24	0.23	0.27	0.28	0.26	0.27	0.2	-	-	-

The GPRNA profile in site 1 (Fig.5.1.) presents a clear peak of amplitude at meter 90. This high scattering zone, ranges from meter 40 to meter 100 approximately and we assume that probably correspond to the flood plane of the torrent. Comparing H/V predominant periods (Fig.5.1.) with the patterns obtained in GPRNA, the maximum values are obtained in high scattering area. Indeed, the greatest value is obtained in point 5 situated at meter 80 of the profile, close to the maximum of GPRNA. The difference between predominant period obtained in this point and the next one is about 42% in a distance of only 25 meters. Predominant periods remain between 1.37 s and 1.57 s outside this high scattering area.

In site 2, two peaks are observed and are continuous along almost the whole profile. Only point 4 has a second peak at a period significantly greater than the other measurements. First peak remains almost constant between 0.26 s and 0.30 s for all the points. GPRNA shows a high scattering zone between meters 65 and 130 of the profile, with a maximum situated in meter 80. However, the point 4 is not situated near the maximum but in meter 127.

For Site 3 GPRNA shows high scattering from meter 15 to meter 100 of the GPR profile. We assume this area as the flood plane of the torrent. Farther, a low scattering area appears from meter 150 and lasts almost until the end of the profile. Between these two zones there is a transition zone, where GPRNA reaches medium values. H/V results present a splitting of the predominant period in two when approaching the transition zone, and along the flood plane.

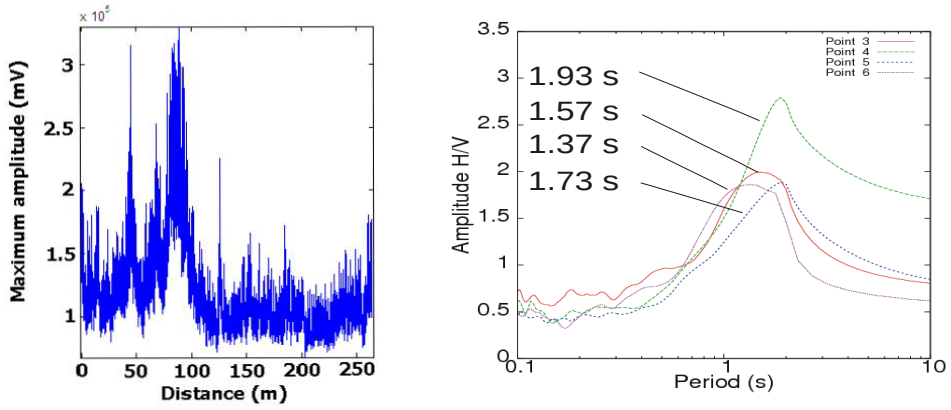

Figure 5.1. Results for site 1. Left: Computed GPR Maximum amplitude. Right: H/V curves for points 3, 4, 5 and 6.

Functions U_3 for two REMI profiles in Sites 2 and 3 are presented in Fig.5.3. For a total horizontally layered medium, we expect no changes between sensors. In site 2, the zone of high scattering almost no overlaps the REMI array. In this case the shape and amplitudes of the curves U_3 are similar for all the sensors. For site 3, sensor 1 and the last sensors (17-24) maintains a similar pattern shape, meanwhile sensors situated in high scattering area (2-12) are in general more variable. In transition area, the behavior of the U_3 functions is a mix between the two cases.

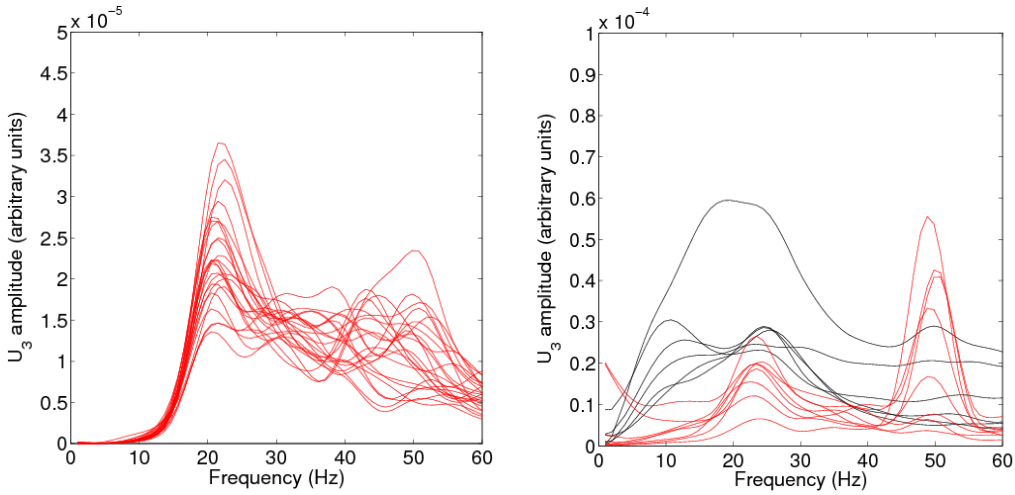

Figure 5.3. U_3 functions for two REMI arrays. Left: U_3 functions for all sensors of site 2. Right: U_3 functions for site 3; in black: sensors 2 to 7 and in red: sensors 17-24.

Based in the results obtained for U_3 functions, the hypothesis of a horizontally layered medium is assumed for subsoil at Site 2. In site 3, we assume two different 1D configurations; one for subsoil under sensors 2 to 12 (for flood plane area) and other for subsoil under sensors 17-24 (for sensors outside). For each one of these assumed 1D configurations, a simultaneous model response fitting is carried out using both the dispersion curve and H/V curves. The resultant models and their responses are presented in Fig. 5.4.

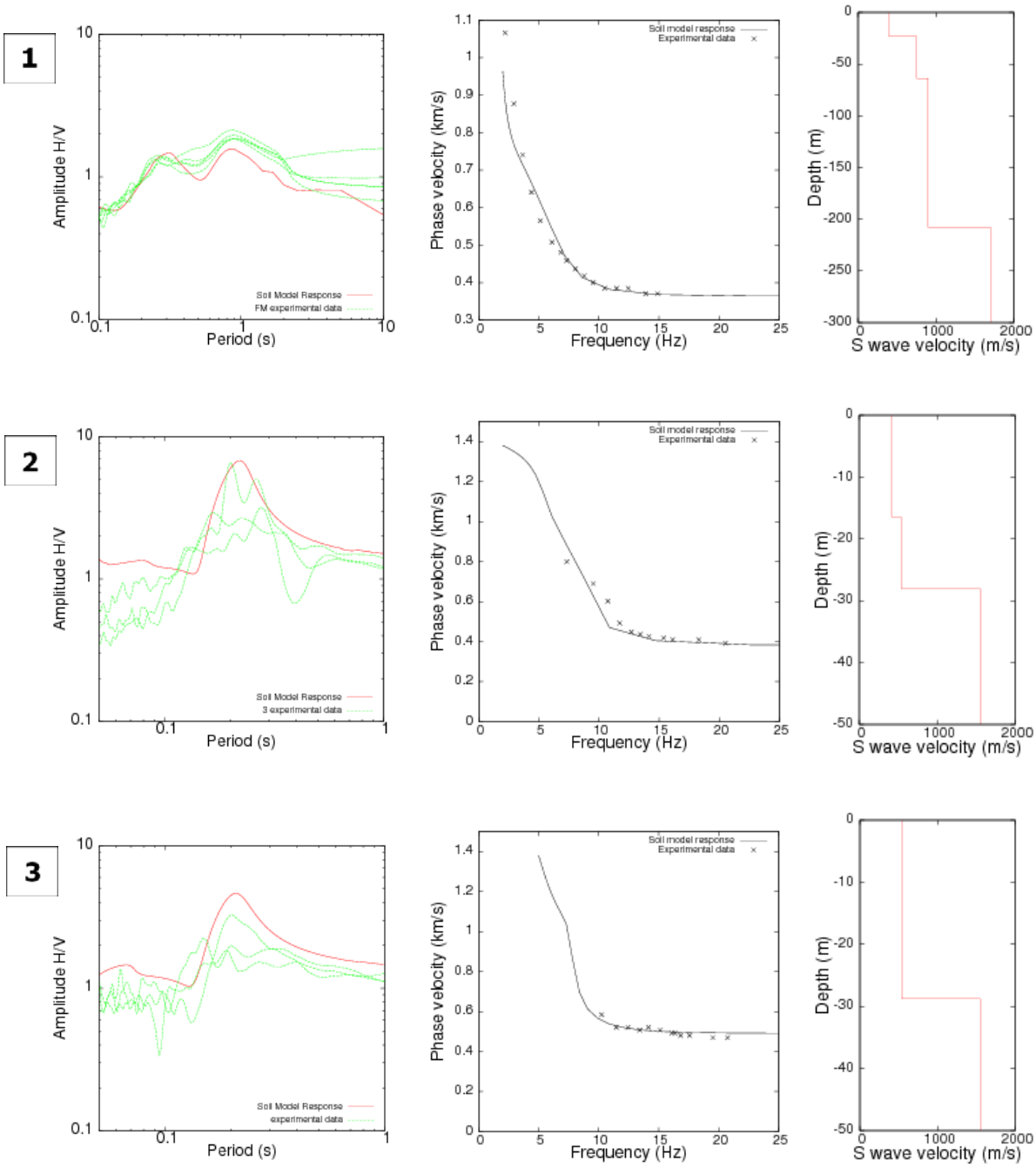

Figure 5.4. Soil model response fitting. (1) Site 2. Left: In green, experimental H/V for points 5, 6, 7, 8 and 9. In red: H/V model response. Center: Black line: model dispersion curve. In points: experimental dispersion curve picks. Right: V_S model. (2) Site 3, flood plane area (sensors 2-12). Left: In green, experimental H/V for points 3, 5 and 6. In red: H/V model response. Center: Black line: model dispersion curve. In points: experimental dispersion curve picks. Right: V_S model. (3) Site 3, outside plane floor area (sensors 17-24). Left: In green, experimental H/V for points 1, 8 and 9. In red: H/V model response. Center: Black line: model dispersion curve. In points: experimental dispersion curve picks. Right: V_S model.

6. DISCUSSION AND CONCLUSIONS

The main aim of the present work was to develop a methodology to identify geological shallow structures which can introduce variations in seismic soil response and to study their effects. To test it, we applied this technique at three sites on Barcelona where this kind of structures usually exist. In addition, REMI array have been carried out in two of the sites.

The obtained results reveal the need of taking into account these lateral changes. Changes of up to 42% for predominant period values appear for short distances (less than 50 meters). Microzonation maps often take representative points at distances of more than 100 meters and, clearly, these effects are not detectable. Selecting a more intensive grid in microzonation when necessary, may be the solution to avoid unexpected damage in buildings.

Thus, the accurate positioning of the paleochannels and torrents under the city becomes one of the important steps in the presented methodology. Even in many cases the information about these structures could be found in geotechnical maps and specialized bibliography, the exact position is not properly defined or misplaced because of the old data. Detailed information could be obtained by means of boreholes. However, holes are inadequate unless just on the structure. For a soil response purposes, it is more important to take into account the flood plane area than the thin line often showed in maps. It is interesting to point out the differences between the position where we are detecting the channels and the location given by different sources. In this sense, bibliography may help to determine roughly where these structures are expected but, for our purposes, it is important to know exactly where they appear. Our evaluation seems to indicate that GPR could be a useful tool to detect quick changes in the shallow geology. Probably deeper geological structures, which are not detected by means of GPR, are not associated to local changes but to big size structures. Notwithstanding, sometimes it is difficult to distinguish between scattering and reflectors by direct inspection of the raw GPR data. Computing GPRNA is most likely a good option to evaluate the effect of the scattering because reflections due to shallow anomalies are not considered in the time window and corrections due to geometrical spreading and ground absorption are applied. GPRNA presents better correlation with the position of torrents and paleochannels emplacement than other GPR data analysis, as the study of the average corrected amplitude, being only considered the reflection in ground discontinuities. However, as results show, not all the GPRNA changes involve a variation in the predominant period. At this point, it is important to remark that electromagnetic waves used in GPR are sensitive to different physic features of the medium that the seismic waves. Also, external clutter due to electromagnetic noise must be considered because the appearance on GPR data is similar to the scattering effect.

Not all the channels or torrents have the same effect on the soil response. As it can be seen in the three cases studied, there are differences both in the magnitude of the predominant period change and in its characteristics. Differences in the shear velocity contrast, the thickness, the consolidation of the fill material, the presence of water etc. are factors which influence the change. In our case, the lower reaches of the torrents (site 1) mainly have bigger banks, more thickness and in consequence greater quantity of fill materials but with low contrast with outside materials. So, lower reaches should produce, in a wide area, greater and smoother changes in the predominant period. Moreover we found that for shallow channel (site 3), the predominant period peak splits in two peaks in the transition zone as if H/V presents the effect of both inside and outside. In site 2, H/V peaks are almost constant on period. Only point 4 presents an anomalous greater period for the second peak. However, this particular measure presents low stability between windows and may be unreliable.

On the other hand, the diffuse field theory has been applied in order to find the H/V response for a one-dimensional shear velocity model. We have fitted simultaneously the model response for experimental H/V ratio and dispersion curves. For all the cases, the fitting process has been done iterating manually and simultaneously for both data, since the inversion algorithm is not implemented. In this sense, the model obtained is surely not the best one but enough. The diffuse field theory has also been applied to validate the applicability of one-dimensional hypothesis. In site 2, we can assume

an horizontally layered medium. For this case, it has been feasible to retrieve a compatible model with both experimental H/V and dispersion curve. In site 3, however, autocorrelations point out the need of split the REMI array in two parts. So, two different one-dimensional models are tested. In site 3, fitted models are less accurate than in site 2, probably due to boundary effects. Then, it seems that to split a 2D structure in different one-dimensional parts leads to an approximated solution. Notwithstanding, the lateral effects induced by the lateral change are not negligible.

Geotechnical soundings and geological maps are useful in most cases to determine roughly the expected predominant period values. This previous knowledge can help to determine the recording time. Also, geotechnical soundings, especially layer thickness, may help to obtain an initial model for numerical simulation. Unfortunately, most of the soundings are not deep enough.

As a general conclusion, nanozonation importance has been highlighted for seismic risk. Geological lateral changes can often be related with high variation of soil response and must be considered in order to obtain accurate soil site and seismic risk maps.

AKCNOWLEDGEMENT

This work has been partially funded by the Spanish Government and with FEDER funds, through the research projects CGL2008-00869/BTE and CGL2011-23621. The first author has a FPI grant funded by the Spanish Government. We thank "Geological Institute of Catalunya" (IGC) and "Cartographic Institute of Catalunya" for the facility to consult soundings and maps.

REFERENCES

Alfaro, A., Pujades, L.G., Goula, X., Susagna, T., Navarro, M., Sanchez, J. and Canas, J.A. (2001). Preliminary Map of Soil's Predominant Periods In Barcelona Using Microtremors. *Pure Appl. Geophys.* **158**, 2499-2511.

Anonymous. (1935). Pla de la ciutat de Barcelona 1:10 000. RM 244413. (in catalan).

Arandes, R. (1998). Hidrogeología del pla de Barcelona (in catalan). *Ajuntament de Barcelona*, Barcelona. Spain.

Bard, P.-Y. (2008). The H/V technique: capabilities and limitations based on the results of the SESAME project. *Foreword. Bull. Earthq. Eng.*, **6**, 1-2.

Cadet H. (2007). Utilisation combinée des méthodes basées sur le bruit de fond dans le cadre du microzonage sismique. *Phd. Thesis. Université J. Fourier*, Grenoble, France. (in french).

Cadet, H., Macau, A., Benjumea, B., Bellmunt, F. and Figueras, S. (2011). From ambient noise recordings to site effect assessment: The case study of Barcelona microzonation. *Soil Dynamics and Earthquake Engineering* **31**, 271-281.

Caselles J.O., Pérez-Gracia V., Franklin R., Pujades L.G., Navarro M., Clapes J., Canas J.A. and García F. (2010). Applying the H/V Method to Dense Cities. A Case Study of Valencia City. *Journal of Earthquake Engineering* **14:2**, 192 – 210.

Cerda, I. (1855). Pla dels voltants de la Ciutat de Barcelona. (in catalan).

Cid, J., Susagna, T., Goula, X., Chavarria, L., Figueras, S., Fleta, J., Casas, A. and Roca, A. (2001). Seismic Zonation of Barcelona Based on Numerical Simulation of Site Effects. *Pure appl. Geophys.* **158**, 2559-1577.

D'Amico, V., Albarello, D. and Mucciarelli, M. (2002). Validation through HVSR measurements of a method for the quick detection of site amplification effects from intensity data: an application to a seismic area in Northern Italy. *Soil Dynamics and Earthquake Engineering* **22**, 475-483.

D'Amico, V., Picozzi, M., Baliva, F. & Albarello, D. (2008). Ambient Noise measurements for preliminary site-effects characterization in the urban area of Florence. *Bull. Seism. Soc. Am.* **98:3**, 1373–1388, doi:10.1785/0120070231

Gosar, A. and Martinec, M. (2009). Microtremos HVSR study of site effects in the Ilirska Bristica town area (S. Slovenia). *Journal of Earthquake Engineering* **13**, 50-67.

Louie, J. N. (2001). Faster, better: shear-wave velocity to 100 meters depth from refraction microtremor arrays. *Bull. Seism. Soc. Am.* **91**, 347-364

Lunedei, E., and Albarello, D. (2010). Theoretical HVSR curves from full wavefield modelling of ambient vibrations in a weakly dissipative layered Earth. *Geophys. J. Int.* **181**, 1093-1108. doi: 10.1111/j.1365-246X.2010.04560.x

Luzón, F., Almendros, J. and García-Jerez, A. (2011). Shallow structure of Deception Island, Antarctica, from correlations of ambient noise on a set of dense seismic arrays. *Geophys. J. Int.* **185**, 737-748

Nakamura, Y. (1989). A method for dynamic characteristics estimation of subsurface using microtremor on the ground surface. *Quaterly Rep. Railway Tech. Res. Inst.* **30:1**, 25-30.

Navarro, M., Enomoto, T., Sanchez, F.J., Matsuda, I., Iwatate, T., Posadas, A.M., Luzón, F., Vidal, F. and Seo, K. (2001). Surface Soil Effects Using Short-Period Microtremor Observations In Almeria City, Southern Spain. *Pure and Applied Geophysics* **158**, 2481-2497.

Parcerisa, D. (2002). Petrologia i diagènesi en sediments de l'Oligocè superior i del Miocè inferior i mitjà de la Depressió del Vallès i del Pla de Barcelona. Evolució de l'area font i dinàmica dels fluids. *Phd. Thesis. Universitat Autònoma de Barcelona.* Barcelona, Spain (in catalan).

Perez-Gracia, V, Caselles, O., Salinas, V., Pujades, L.G. and Clapés, J. (2010). GPR applications in dense cities: detection of paleochannels and infilled torrents in Barcelona. *XIII International Conference on Ground Penetrating Radar*, 434-438.

Perton, M., Sánchez-Sesma, F. J., Rodríguez-Castellanos, A., Campillo, M. and Weaver, R. L.. (2009). Two perspectives on equipartition in diffuse elastic fields in three dimensions. *J. Acoust. Soc. Am.* **126**, 1125-1130.

Pliz, M., Parolai, S., Leyton, F., Campos, J., and Zschau, J. (2009). A comparison of site response techniques using earthquake data and ambient seismic noise analysis in the large urban areas of Santiago de Chile. *Geophys. J. Int.* **178:2**, 713-728.

Roux, P., Sabra, K. G., Gerstoft, P., Kuperman, W. A. and Fehler, M.C. (2005). P-waves from cross-correlation of seismic noise. *Geophys. Res. Lett.* **32**, L19393. doi: 10.1029/2005GL023803.

Sabra, K., Gerstoft, G. P., Roux, P., Kuperman, W. A. and Fehler, M. C. (2005). Extracting time-domain Green's function estimates from ambient seismic noise. *Geophys. Res. Lett.* **32**, L03310. doi: 10.10292004GL021862.

Sánchez-Sesma, F. J. and Campillo, M. (2006). Retrieval of the Green function from cross-correlation: the canonical elastic problem. *Bull. Seism. Soc. Am.* **96**, 1182-1191.

Sánchez-Sesma, F. J., Pérez-Ruiz, J. A., Campillo, M. and Luzón, F. (2006). The elastodynamic 2D Green function retrieval from cross-correlation: the canonical problem. *Geophys. Res. Lett.* **33**, L13305. doi: 10.1029/2006GL026454.

Sánchez-Sesma, F. J., Pérez-Ruiz, J. A., Luzón, F. Campillo, M. and Rodriguez-Castellanos, A. (2008). Diffuse fields in dynamic elasticity. *Wave Motion* **45**, 641-654.

Sánchez-Sesma, F. J., Rodríguez, M., Iturrarán-Viveros, U., Luzón, F., Campillo, M., Margerin, L., García-Jerez, A., Suarez, M., Santoyo, M. A. and Rodríguez-Castellanos, A. (2011). A theory for microtremor H/V spectral ratio: Application for a layered medium. *Geophys. J. Int.* **186:1**, 221-225.

Shapiro, N. M. and Campillo, M. (2004). Emergence of broadband Rayleigh waves from correlation of the ambient seismic noise. *Geophys. Res. Lett.* **31**, L07614. doi: 10.1029/2004GL019491.

Snieder, R. (2004). Extracting Green's function from the correlations of coda waves: a derivation based on stationary phase. *Phys. Rev. E* **69**, 046610.1-046610.8.

Vazquez, L. (1861). Proyecto de ensanche de la ciudad de Barcelona y su puerto aprovado por el gobierno de S.M. (in spanish).

Ventayol, A., Palau, J., Céspedes, A., Barberá, M., Pascual, C., Roset, R., Fabrellas, I., Fernádez, J.J., Marturià, J., Cid, J., Parra, E., Buxó, P., Cabrera, M., Galindo, J. and Bley, G. (2000). Geotechnical Map of Barcelona 1:25000 (in catalan). *Cartographic Institute of Catalonia*. Barcelona.

Weaver, R. L. and Lobkis, O. I. (2004). Diffuse Fields in open systems and the emergence of the Green's function. *J. Acoust. Soc. Am.* **116**, 2731-2734.